FROST-INDUCED BLACK ICE PREDICTION USING ATMOSPHERIC DATA

Jinhwan Jang
Highway and Transport Research Department, Korea Institute of Civil Engineering and Building Technology, 283 Goyangdae-Ro, Illsanseo-Gu, Goyang-Si, Gyeonggi-Do 411-712, Republic of Korea,
jhjang@kict.re.kr, 0000-0002-5529-5913

Summary

Given the high frequency of accidents that occur on icy roads at night, it would be beneficial to alert road managers and drivers about the most hazardous locations. The present study examined well-established prediction techniques such as deep neural network (DNN), random forest (RF), and support vector machine (SVM), with the aim of predicting frost-induced night icing on four different bridges on the National Highways in Korea using atmospheric data. The input data for the models consisted of relative humidity, air temperature, dew point temperature, and the differences in air temperature and humidity between two consecutive days. As a result, DNN and RF performed equally well with an accuracy of 95%, followed by SVM with an accuracy of 92.5%. Given the growing emphasis on preventive maintenance, these developed forecasting models can be applied proactively as an anti-icing measure, ultimately enhancing traffic safety on winter roads.

Keywords: Black Ice, Prediction, Deep Neural Network, Random Forest, Support Vector Machine

INTRODUCTION

Numerous traffic collisions take place on slick roadways. A study reveals that in the United States, accidents on slippery roads result in 1,300 fatalities and 13,735 injuries every year [1]. A Swedish report stated that a mere 14% of motorists effectively speed up and slow down when driving on slippery surfaces [2]. Research from Portugal suggests that the likelihood of a crash on icy roads is nine to ten times higher than on dry surfaces [3]. Based on data from South Korea, 198 deaths have resulted from 6,502 incidents on slippery roads over a five-year period. In 2019, South Korea experienced a devastating accident on an icy road caused by freezing rain, which led to seven fatalities and numerous injuries; a similar event occurred again in 2022.

Also, Korean government directed road maintenance organizations to measure pavement temperatures during nighttime road maintenance patrols, using these measurements as a basis for anti-icing efforts [4]. Since atmospheric sensors are often located far from roads, road temperatures cannot be dependably monitored. Additionally, significant fluctuations in surface temperatures, even on short segments of roadways, limit the usefulness of atmospheric temperature data for anti-icing measures [5]. Consequently, continuous measurement of pavement temperatures along roadways is essential for successful anti-icing operations against black ice.

Typically, snow removal is carried out based on weather forecasts, meaning snow plows are used to clear snow and/or spread chemicals during or just before (1-3 hours) snowfall. However, due to the lack of black ice forecasts in Korea, maintenance staff must perform daily patrols along roads, placing a considerable burden on them.

To tackle this issue, this study developed black ice forecasting models to improve the efficiency of anti-icing efforts, particularly for frost-caused black ice. Three widely recognized machine learning algorithms - deep

neural network (DNN), random forest (RF), and support vector machine (SVM) - were explored using atmospheric. With these forecasting models, nighttime black ice can be predicted using daytime weather forecasts, allowing maintenance personnel to carry out anti-icing activities (patrolling and applying chemicals) only when black ice is anticipated.

METHOD

Methods in Previous Studies

Black ice can form due to various reasons [6], including the freezing of melted snow overnight, rain that freezes on negatively-tempered pavement, and frost bonding with the road surface. The first two causes can be predicted with atmospheric weather forecasting since they are caused by snow or rain. However, the last cause can only be detected through regular road maintenance patrols [7].

To predict black ice, physical models and regression analysis have primarily been used. Physical models use a surface energy balance model based on heat conduction, convection, radiation, and vapor movement estimates to predict pavement temperature [8-11]. Regression models predict pavement temperature using different data, such as atmospheric data, geometry, and air temperature from probe cars [12-14]. However, both types of models have limitations. Physical models require hard data, such as pavement thickness, heat transfer rate of pavement material, and heat flux, which are not always obtainable, indicating that atmospheric data and pavement temperature alone cannot effectively forecast black ice. Regression models are relatively simple to understand but struggle with predicting variables that have a non-linear correlation. Thus, three machine learning models including DNN, RF, and SVM were utilized for this study to overcome the limitations of the previous methods.

Baseline Data Generation for Evaluating Estimated Black Ice Information

In order to evaluate the accuracy of the predicted black ice information, baseline data is necessary. While using a reference device to measure road surface status would be the most reliable and straightforward method, it was not practical for this particular study due to the associated labor requirements, cost, and the need to acquire the device. Instead, a physical principle expressed in equation (1) was used, which states that frost on a pavement forms when the pavement temperature is not only negative, but also lower than the dew point.

$$T_p \leq 0℃ \; and \; T_p \leq T_d \quad (1)$$

where Tp = pavement temperature and Td = dew point temperature.

The dew point temperature refers to the temperature at which vapor becomes saturated, leading to the formation of fog or frost and causing the relative humidity to reach 100%. The calculation of the dew point temperature is often done using the Magnus formula, which is a widely used method for this purpose [15]. The formula calculates the saturation vapor pressure (EW) over liquid water at a specific temperature (T) using equation (2).

$$EW = \alpha \cdot e^{\left(\frac{\beta \cdot T}{\lambda + T}\right)} \quad (2)$$

Equation (2) involves the use of parameters α (6.112 hPa), β (17.62), and λ (243.12℃). By rearranging the terms in equation (2), the dew point (Td) can be expressed as equation (3) in terms of vapor pressure.

$$T_d = \frac{\lambda \cdot \ln\left(\frac{E}{\alpha}\right)}{\beta - ln\left(\frac{E}{\alpha}\right)} \quad (3)$$

If we substitute the definition of relative humidity (E = RH*EW/100) into equation (3), we can obtain the dew point (Td) using both atmospheric temperature (T) and relative humidity (RH), as shown in equation (4).

$$T_d(T,\ RH) = \frac{\lambda \cdot \left[\ln\left(\frac{RH}{100}\right) + \frac{\beta \cdot T}{\lambda + T}\right]}{\beta - \left[ln\left(\frac{RH}{100}\right) + \frac{\beta \cdot T}{\lambda + T}\right]} \quad (4)$$

Equations (2)-(4) utilize the Magnus formula, which is widely accepted as a method to estimate the dew point temperature based on the atmospheric temperature and relative humidity, with an error rate of around 0.35℃ [16].

In order to verify the accuracy of the Magnus formula, a wintertime road segment was patrolled. The observation was made that frost-induced black ice occurred (on the left) when the conditions for frost formation were met, while no black ice was observed (on the right) when those conditions were not met, as illustrated in Figure 1.

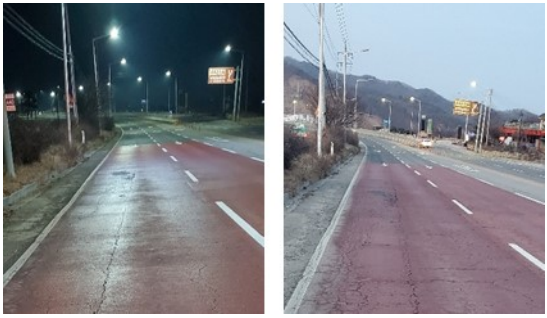

Figure 1 Pavement with frost (left) and without frost (right).

DATA

Data Collection

Pavement Temperature and Atmospheric Data

For this study, road maintenance vehicles are equipped with a road surface temperature sensor (Figure 2) that uses an infrared thermometer to measure the temperature of the pavement (Figure 3). The sensor can measure the temperature every 0.2 seconds while the vehicle is in motion. The sensor has a very narrow half-angle of 5°, which makes it highly

accurate when measuring surface temperature [17]. The sensor has an accuracy of ±0.3℃ at 0℃. Also, corresponding atmospheric data at the same time were obtained from the nearest weather station.

Figure 2 Pavement temperature sensor.

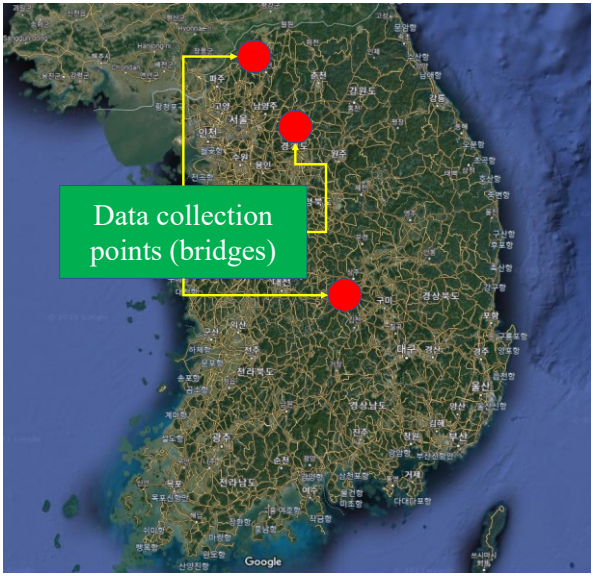

Figure 3 Data collection sites.

Preprocessing of Pavement Temperature Data

To apply the collected data effectively to de-icing activities, it was necessary to aggregate the data by roadway segment. To accomplish this, the Korean government established a standard node-link system (Figure 4), which divides the entire public highway network into nodes and links based on roadway features such as bridge, tunnel, overpass, underpass, intersection, number of lanes, etc. Since the pavement temperature varies by roadway type, aggregation by the node-link system is considered to be reasonable and effective.

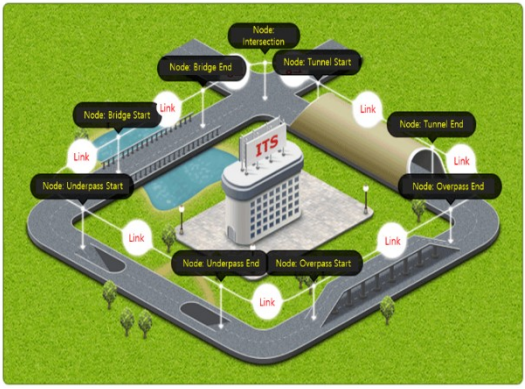

Figure 4 Standard node-link system of Korea.

To process the pavement temperature, a standard link was used to aggregate the data into a single median value as a measure of central tendency. However, since pavement temperature measurements collected from moving vehicles may contain outliers due to various factors like debris on the pavement, driving on the shoulder lane, intermittent stops during patrolling, etc., a prudent aggregation method was required to mitigate any unexpected consequences caused by these outliers. Among the three measures of central tendency (mean, median, and mode), the median was selected because it is less susceptible to outlying observations [18-20].

Relationship between Pavement Temperature and Atmospheric Data

<Figure 5> shows a graph of the pavement temperature and air temperature collected at one of the three points mentioned above. Similar patterns were observed at the other two points. Overall, the bridge temperature was observed to be lower than the air temperature, and the variability was observed to be greater in the air temperature. As shown in <Table 1> and <Figure 6>, the average temperature was about 2 ℃ lower for the bridge temperature compared to the air temperature, but the maximum temperature was about 4 ℃ higher. The minimum temperature was about 2 ℃ lower for the air temperature compared to the pavement temperature. Unlike the air temperature, which fluctuates significantly with air flow, the pavement temperature is thought to have relatively low variability due to geothermal and latent heat of the structure.

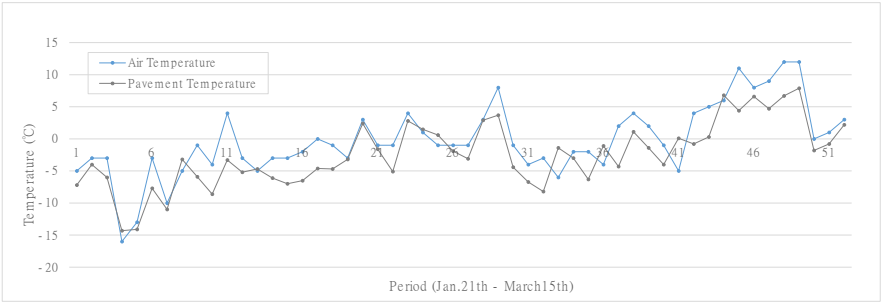

Figure 5 Air temperature vs. pavement temperature.

Table 1 Statistics of pavement (bridge) and air temperature

Statistics	Air tem.	Pav. (Bridge) temp.
Mean	-0.30	-2.47
Standard deviation	5.56	5.01
Minimum	-16.00	-14.30
25 %	-3.00	-5.93
50 %	-1.00	-3.15
75 %	3.00	0.73
Maximum	12.00	7.90

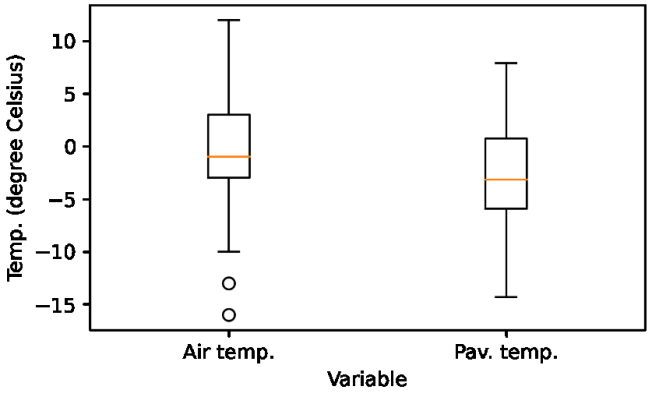

Figure 6 Boxplot of air and pavement temperature.

<Figure 7> shows the temperature and humidity characteristics during frost formation. The point indicated by the round points in red in <Figure 7 (b)> is when frost formation occurs according to equation (1) (when the pavement temperature is below freezing and lower than the dew point temperature). Examining the temperature and humidity patterns in <Figure 7 (a)> during frost formation, it can be seen that in most cases, temperature and humidity rise simultaneously. Additionally, it can be seen that even if the air temperature is above freezing, frost can occur when the pavement temperature is lower than the freezing point of 0 ℃. The temperature difference between the air temperature and bridge temperature was observed to be up to 4 degrees. From the analysis conducted, it can be deduced that during winter, frost is more likely to form when temperatures are increasing rather than decreasing, as long as the pavement temperature remains below 0 ℃.

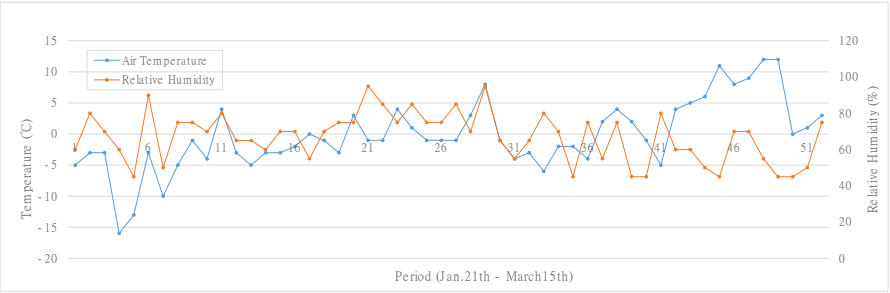

(a) Air temperature vs. relative humidity

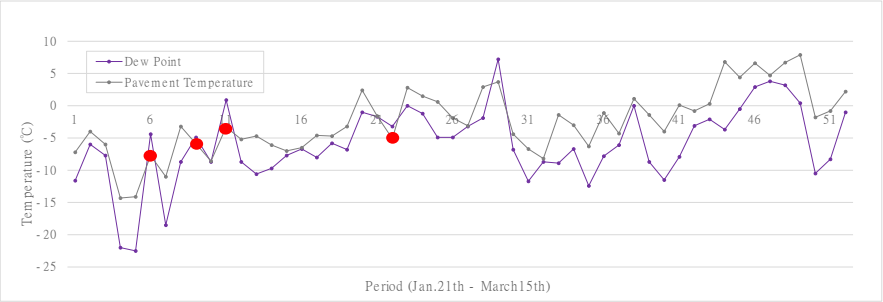

(b) Dew point temperature vs. pavement temperature

Figure 7 Cases of frost-induced black ice formation.

BLACK ICE PREDICTION

Building Blocks of Machine Learning Models

Based on the above-investigated results, we developed a nighttime black ice prediction model using atmospheric data. The input data for the machine learning models consisted of temperature, humidity, temperature difference from the previous and following days, humidity difference from the previous and following days, and dew point temperature, which were collected over a two-year period at the three points mentioned earlier. The baseline data were generated using equations (1-4) with the input data and pavement temperature data collected by patrol vehicles. We employed three well-known prediction models, namely DNN, RF, and SVM, which are known

to have generally superior performance. <Figure 8> depicts the building blocks for the three models. Since the scale of each input data was different, we standardized the data using a standard scaler before training the models. The training and test sets were classified into a 7:3 ratio, and the dry/icing data ratios of the raw data were applied during classification to ensure a balanced distribution in both sets. The total data used for analysis consisted of 397 days, including 193 days of icy and 204 days of dry conditions.

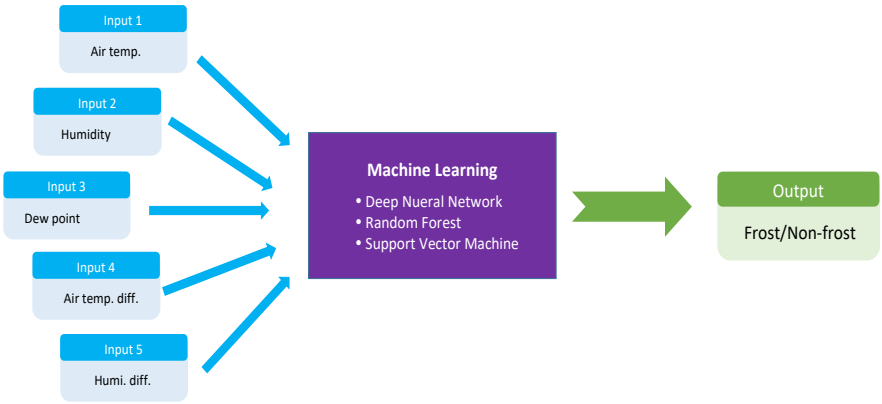

Figure 8 Building blocks of machine learning models.

Deep Neural Network

The DNN model was built using the Tensorflow Keras platform. As shown in <Table 2>, the model had a 30x20 hidden layer and a total of 821 parameters. The optimal number of hidden layers was determined with error-and-trial process [21]. The rectified linear unit activation function was used, and the Adam optimizer was applied with 50 epochs. <Figure 9> shows the training process of the built model, using accuracy as the evaluation metric. As shown in <Table 3>, the predicted results of the model demonstrated overall satisfactory performance, with a particularly notable 100% prediction rate for icing conditions. Thus, the performance of the model was deemed satisfactory."

Table 2 Constructed deep neural network model

Layer (type)	Output Shape	Param #
dense (Dense)	(None, 30)	180
dense_1 (Dense)	(None, 20)	620
dense_2 (Dense)	(None, 1)	21
Total params: 821		
Trainable params: 821		
Non-trainable params: 0		

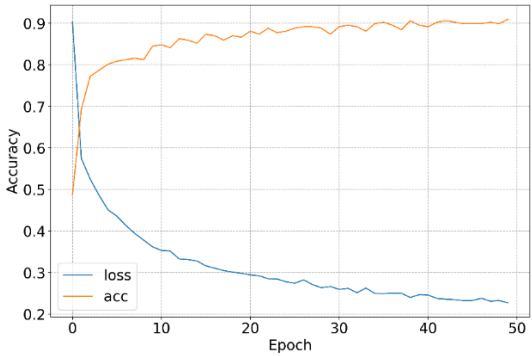

Figure 9 Learning process of deep neural network model.

Table 3 Confusion matrix of deep neural network model

Classification		Prediction	
		Dry	Icy
Baseline	Dry	0.919	0.081
	Icy	0.000	1.000

Random Forest

The Random Forest model was constructed using the Python language. Random Forest is a prediction model that averages multiple decision trees, so it is crucial to determine the optimal number of decision trees. To achieve this, while keeping other parameters fixed at constant

values, decision trees ranging from 1 to 50 were investigated using accuracy as the evaluation metric.

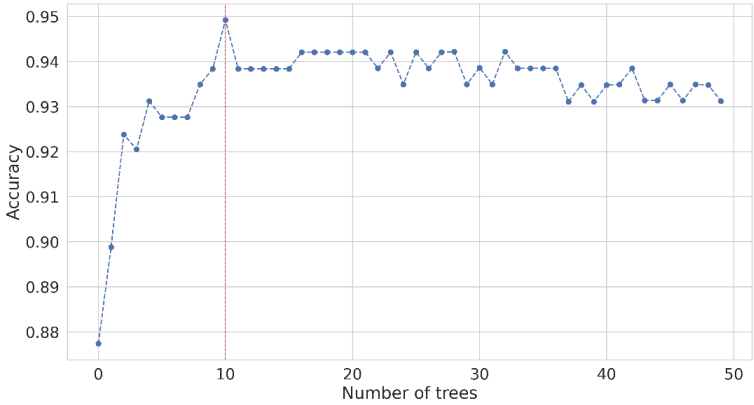

Figure 10 Searching process of the optimal number of trees.

Table 4 Feature importance for random forest model

Features	Humidity	Air temp. diff.	Dew point	Air temp.	Humi. diff.
Gini-Importance	0.437	0.236	0.155	0.086	0.086

Consequently, the optimal number of decision trees was determined to be 11, as depicted in <Figure 10>. Other parameters, excluding decision trees, were estimated using the "GridSearchCV" library. The resulting optimal parameters were determined to be {‘criterion’: entropy, ‘max_depth’: 10, 'max_features': auto, 'max_leaf_nodes': 30, and 'n_estimators': 12}. Unlike other models, the RF model can calculate the importance of each input variable. Analyzing the widely used Gini-importance for impurity measurement, it can be seen from <Table 4> that humidity and air temperature difference between consecutive days have the highest importance. This is consistent with the findings in <Figure 7>. As seen in <Table 5>, the performance of the model is also excellent.

Table 5 Confusion matrix of random forest model

Classification		Prediction	
		Dry	Icy
Baseline	Dry	0.935	0.065
	Icy	0.034	0.966

Support Vector Machine

The SVM model was also constructed using the Python language, similar to the RF model, and there are several parameters for model optimization in SVM as well. When training an SVM model, the performance of the model heavily depends on the parameter settings

The optimal parameters were determined using the GridSearchCV library in this analysis, and the resulting values were {'C': 100, 'gamma': 'auto', and 'kernel': 'rbf'}. <Table 6> shows the results predicted using the optimal parameters. Although the performance is somewhat lower than that of DNN and RF, the overall performance is satisfactory, with an accuracy of over 0.9.

Table 6 Confusion matrix of support vector machine model

Classification		Prediction	
		Dry	Icy
Baseline	Dry	0.887	0.113
	Icy	0.034	0.966

DISCUSSIONS

<Table 7> is a comparison table for three different models. Performance comparison was done using accuracy, precision, recall, and F1 score, which, as expressed in equations (5-8), are commonly used for evaluating machine learning models. DNN and RF showed the same

performance, but in the case of the F1 score, DNN was higher. Since the recall of DNN is 100%, there were no cases of predicting an icy surface as a dry surface, making it more satisfactory compared to other models.

$$Accuracy = \frac{True\ Positive+True\ Negative}{True\ Positive+True\ Negative+False\ Positive+False\ Negative} \quad (5)$$

$$Precision = \frac{True\ Positive}{True\ Positive+False\ Positive} \quad (6)$$

$$Recall = \frac{True\ Positive}{True\ Positive+False\ Nagative} \quad (7)$$

$$F1\ Score = \frac{2}{\frac{1}{Precision}+\frac{1}{Recall}} \quad (8)$$

Table 7 Model performance comparison

Model	Accuracy	Precison	Recall	F1 score
DNN	0.950	0.906	1.000	0.951
RF	0.950	0.933	0.966	0.949
SVM	0.925	0.889	0.966	0.926

It should be noted that the baseline data used in this analysis is not the actual surface condition observed in the field, but rather calculated values using road surface temperature and atmospheric data. Even if the conditions for frost formation are met according to physical laws, road icing may not occur in cases of high traffic volume [22]. Nevertheless, the results of this study can be highly valued from the following perspectives. From the viewpoint of road administrators, if icing due to frost is expected, they should perform anti-icing activities. In this regard, the results of this study can be usefully applied to real-world winter road maintenance activities.

CONCLUSIONS AND FUTURE STUDIES

In Korea, as previously stated, accidents caused by black ice (resulting in seven fatalities in 2019 and numerous injuries in 2023) have led

to significant changes in winter road maintenance practices. Recently, field workers have been tasked with daily maintenance patrols throughout the winter season. As a result, field personnel have been requesting an improved patrolling schedule, highlighting the need for the development of nighttime ice predictions.

For snow removal, field personnel can rely on atmospheric weather forecasts, but no such predictive information is available for black ice treatment. Consequently, workers are often compelled to carry out maintenance patrols, even when black ice is not expected. To tackle this issue, three reputable machine learning models were explored to predict nighttime black ice potential, achieving satisfactory results with accuracies above 92%.

Nonetheless, the deep learning models created were evaluated solely based on baseline data derived from a physical principle. In the future, if feasible, baseline data should be gathered from field observations using a device that accurately measures road slipperiness to ensure a more dependable evaluation.

REFERENCES

[1] U.S. FHWA [Online]. Available: https://ops.fhwa.dot.gov/weather/weather_events/snow_ ice .htm

[2] J. Bogren and P. E. Caran. *SRIS-Slippery Road Information System*, Intelligent Vehicle Safety Systems, 2010.

[3] P. Luque, J. Wideberg, and D. Mantars. *ITS to Improve Safety and Efficiency OBD-II and Smartphone Apps*, CreateSpace Independent Publishing Platform, 2013.

[4] Korean Government. Winter Road-Traffic Safety Enhancement Measures (in Korean), 2020.

[5] Mats R., Torbj G., Jorgen B., and Per-Erik J. Ice Formation Detection on Road Surfaces using Infrared Thermometry, *Cold Regions Science and Technology*, Elsevier, Vol. 83–84 (2012), pp. 71–76, 2012.

[6] American Association of State Highway and Transportation Officials. *Update of the AASHTO Guide for Snow and Ice Control*, Transportation Research Borad, 2008.

[7] PIARC Technical Committee. *Snow and Ice Databook 2018*, PIARC, 2018.

[8] Louis-Philippe C. and Yves D. METRo: A New Model for Road-Condition Forecasting in Canada, *Journal of Applied Meteorology*, Vol. 40, American Meteorological Society, pp. 2026-2037, 2001.

[9] Tina M. G., and Eugene S. T. Bridge Frost Prediction by Heat and Mass Transfer Methods, *Journal of Applied Meteorology and Climatology*, Vol. 45, American Meteorological Society, pp. 517-525, 2006.

[10] Claudia D. N., Roberto C., Gianluca A., and Guido B. Thermal mapping as a valuable tool for road weather forecast and winter road maintenance: An example from the Italian Alps, *Proceedings of the Fourth International Conference on Remote Sensing and Geo-information of the Environment*, Cyprus Remote Sensing Society, 2016.

[11] Virve K. *Observing and Forecasting Road Surface Temperatures*, Ph.D. Dissertation, University of Helsinki, Finland, 2019.

[12] Lee C., John E. T. and Andrew V. B. Modelling of Road Surface Temperature from a Geographical Parameter Database (Part 2: Numerical), *Meteorol. Appl.*, Vol. 8, pp. 421–436, 2001.

[13] Veronica B., Adrian R., Tilmann G., and Richard S. Probabilistic Weather Forecasting for Winter Road Maintenance, *Journal of American Statistical Association*, American Statistical Association, Vol. 105, No. 490, pp. 522-537, 2010.

[14] Yumei H., Esben A., Torbjorn G., and Jrgen B. Modeling Road Surface Temperature from Air Temperature and Geographical Parameters—Implication for the Application of Floating Car Data in a Road Weather Forecast Model, *Jour. of Appli. Meteolo. and Clima.*, American Meteorological Society, Vol. 58, pp. 517-525, 2019.

[15] Sonntag D. Vapour Pressure Formulations based on the IST-90 and Psychrometer Formulae, *Z. Meteorol.*, 70 (5), pp. 340-344, 1990.

[16] Paul R. and Paul J. D. Night Icing Potential – Demonstration Project., *Proc. of the 2008 Annual conference of the Transportation Association of Canada*, Transportation Association of Canada, Toronto, Ontario, 20

08.
[17] https://www.apogeeinstruments.com/field-of-view/, Accessed in July, 2022.
[18] Shao J. and Lister P. J. Data Filtering for Thermal Mapping of Road Surface Temperatures, *Meteorol. Appl.*, Vol. 2, pp. 131-135, 1995.
[19] Shao J. and Lister P. J. Data Filtering for Thermal Mapping of Road Surface Temperatures, *Meteorol. Appl.*, Vol. 2, pp. 131-135, 1995.
[20] ASTM International. *Standard Practice for Dealing with Outlying Observations*, E 178 – 08, 2008.
[21] B. R. Temeyer. *Use of an artifificial neural network to predict air temperature, surface temperature, dew point and wind speed for the prediction of frost*, Master's thesis, Iowa State University, 2003.
[22] Gustavsson T. Variation in Road Surface Temperature due to Topography and Wind, *Theor. Appl. Climatol.*, Vol. 41, pp. 227-236, 1990.